Detection of Gravitational Waves from Core-Collapse Supernovae Using Deep Learning

Seiya Sasaoka[1], Yilun Hou[1], Diego Dominguez[1], Suyog Garg[2], Kentaro Somiya[1], Hirotaka Takahashi[3]
Tokyo Tech[1], ICRR[2], Tokyo City Univ. [3]

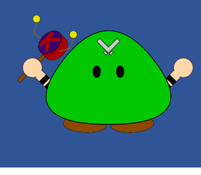

INTRODUCTION

Core-collapse supernovae (CCSNe) are potential sources of gravitational waves (GWs) that could be detected by ground-based interferometric detectors, and their detection and analysis are of great importance for understanding their explosion mechanism. In this study, we applied deep learning to detect GWs from CCSNe. We used phenomenological waveforms with g-mode and SASI to train a model and validated it using waveforms from three-dimensional numerical simulations.

DATASETS

- Signal: phenomenological waveforms

$$h(t) = \underbrace{\exp\left[-\left(\frac{2\pi(t-t_g)}{\sigma_g^2}\right)^2\right]\cos\phi(t)}_{\text{g-mode}} + r\underbrace{\exp\left[-\left(\frac{2\pi(t-t_s)}{\sigma_s^2}\right)^2\right]\sin(2\pi f_s t)}_{\text{SASI}}$$

$$\phi(t) = 2\pi\left(\frac{f_{\max}+f_{\min}}{2}(t-t_g/2) + 0.05\frac{f_{\max}-f_{\min}}{2}\log\left(\cosh\left(\frac{t-t_g/2}{0.05}\right)\right)\right)$$

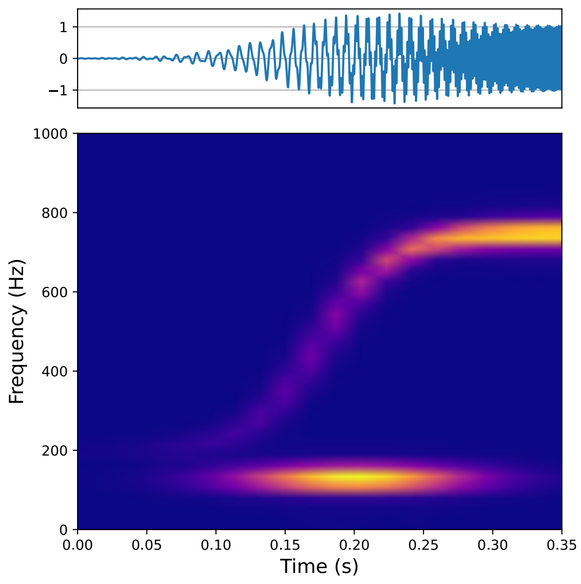

FIG. 1. A phenomenological waveform in time domain and its spectrogram

TABLE I. Range of the parameters of the phenomenological waveforms

		min	max
g-mode	t_g	0.2	0.6
	σ_g^2	0.8	1.3
	$f_{\min}$	150	500
	$f_{\max}$	500	2000
ratio	r	0	1
SASI	t_s	t_g-2	t_g+2
	σ_s^2	0.4	0.7
	f_s	100	150

- Noise
  - ➢ Gaussian

  Produced using power spectral density derived from O3a open data [1] using Welch's method

  - ➢ Real

  Obtained from O3a open data [1]

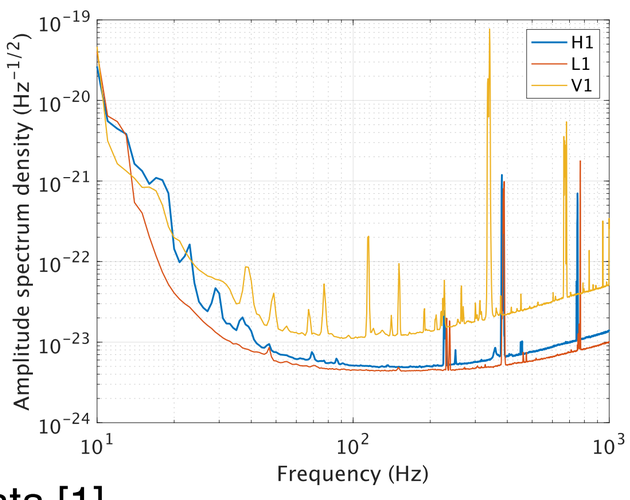

FIG. 2. Estimated Amplitude spectral density of each detector.

- Training data:

  5,000,000 phenomenological waveforms in Gaussian noise and 5,000,000 pure Gaussian noise samples

- Test data:

  We used 3D numerical simulation data from the following papers: Radice 2019 [2], Powell 2019 [3], Powell 2020 [4], and Powell 2021 [5], and generated two test sets: signals in Gaussian noise and those in real noise.

MODEL

We trained two models; the structure is same (Table II), but the **model 1** is trained using waveforms with SASI, and the **model 2** is trained using only waveforms without SASI.

TABLE II. The structure of the convolutional neural network model we used.

Layer	Input	1	2	3	4	5	6	7	8	9
Type		Conv	Conv	Conv	Conv	Conv	Conv	Linear	Linear	Linear
Size	(3,4096)	(16,4033)	(16,992)	(16,961)	(16,310)	(16,295)	(16,140)	64	64	2
Kernel size		64	64	32	32	16	16	-	-	-
Maxpool size		-	4	-	3	-	2	-	-	-
Dropout		0	0	0	0	0	0	0.25	0.25	0
Activation		SiLU	SiLU	SiLU	SiLU	SiLU	SiLU	SiLU	SiLU	Softmax

RESULTS

- Loss curve

After 30 epochs of training, the accuracy of validation set was about 80%.

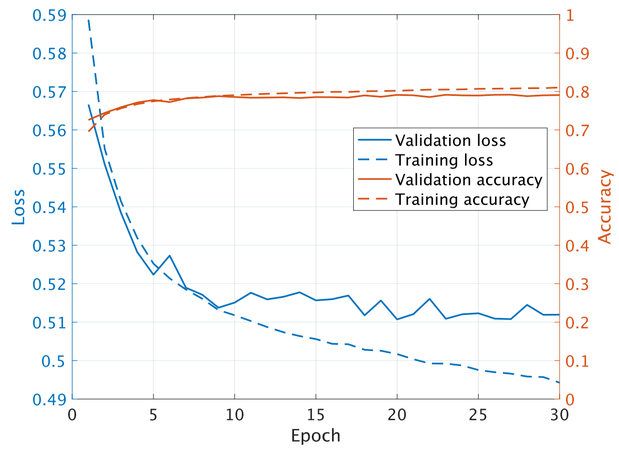

FIG. 3. Accuracy and loss curves.

- Model1 vs. Model2

Figure 4 shows that model 1, trained using signals with SASI, exhibits better detection efficiency for the signals with SASI in Gaussian noise.

Figure 5 shows that model 1, trained with signals with SASI performs better than model 2 for signal with SASI at large distances. This indicates that training a model using SASI works well when detecting small signals.

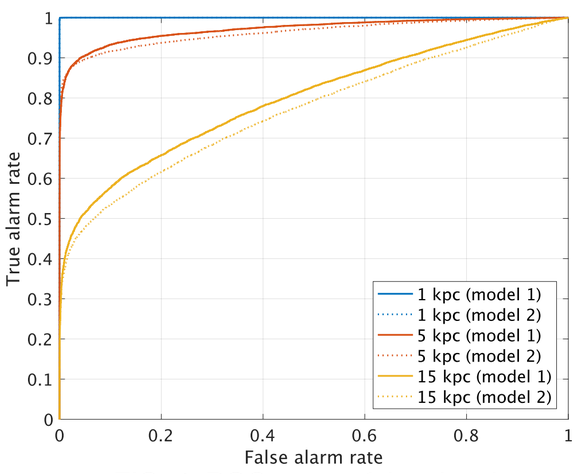

FIG. 4. ROC curve of the signals with SASI in Gaussian noise.

On the other hand, for signals without SASI, there is no much difference between model 1 and model 2 at any distance because the training set of model 1 also includes signals without SASI.

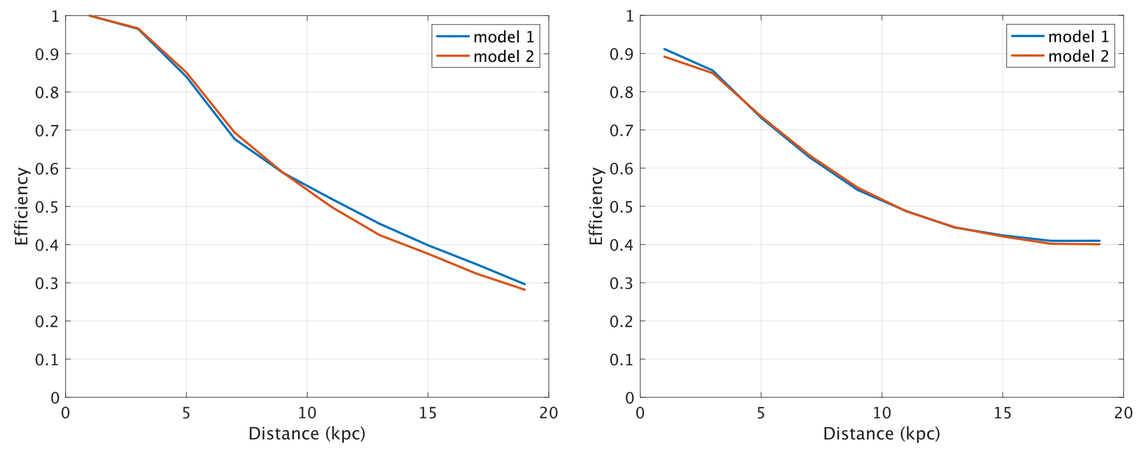

FIG. 5. Detection efficiency vs. distance curve for the signals with SASI (left) and without SASI (right) in Gaussian noise. False alarm rate is fixed to 0.01.

- Gaussian noise vs. Real noise

The efficiency of the model for signals in real noise was expected to be lower than for signals in Gaussian noise due to non-stationary or non-Gaussian noise, but Fig. 6 shows the opposite. We do not know the cause at the moment and would like to continue the investigation.

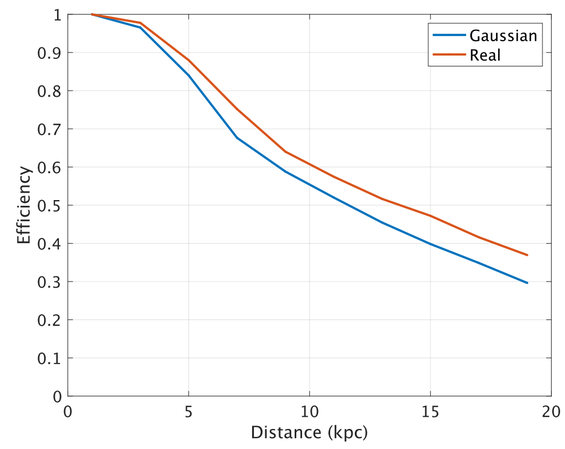

FIG. 6. Detection efficiency vs. distance curve of model 1 for the signals with SASI in Gaussian and real noise.

REFERENCES

[1] GWOSC, The O3a Data Release, https://www.gw-openscience.org/O3/O3a/.
[2] Radice *et al.*, ApJL **876**, L9 (2019).
[3] Powell *et al.*, MNRAS **487**, 1178 (2019).
[4] Powell *et al.*, MNRAS **494**, 4665 (2020).
[5] Powell *et al.*, MNRAS **503**, 2108 (2021).